AGU PUBLICATIONS

Paleoceanography

RESEARCH ARTICLE
10.1002/2016PA003014

Key Points:
- We used the clumped isotope thermometer to measure temperature and seawater $\delta^{18}O$ in Bermuda during the Last Interglacial
- At one locality we found cold temperatures and negative seawater $\delta^{18}O$ values indicative of meltwater reaching subtropical latitudes
- The source of this meltwater may have been the Greenland Ice Sheet, which is sensitive to future global warming

Supporting Information:
- Supporting Information S1
- Data Set S1

Correspondence to:
I. Z. Winkelstern,
ianzw@umich.edu

Citation:
Winkelstern, I. Z., M. P. Rowe, K. C. Lohmann, W. F. Defliese, S. V. Petersen, and A. W. Brewer (2017), Meltwater pulse recorded in Last Interglacial mollusk shells from Bermuda, *Paleoceanography*, *32*, 132–145, doi:10.1002/2016PA003014.

Received 2 AUG 2016
Accepted 29 DEC 2016
Published online 8 FEB 2017

Meltwater pulse recorded in Last Interglacial mollusk shells from Bermuda

Ian Z. Winkelstern[1], Mark P. Rowe[2], Kyger C. Lohmann[1], William F. Defliese[3], Sierra V. Petersen[1], and Aaron W. Brewer[4]

[1]Department of Earth and Environmental Sciences, University of Michigan, Ann Arbor, Michigan, USA, [2]Department of Earth and Planetary Sciences, Birkbeck, University of London, London, UK, [3]Department of Earth, Planetary, and Space Sciences, University of California, Los Angeles, California, USA, [4]Department of Earth and Space Sciences, University of Washington, Seattle, Washington, USA

Abstract The warm climate of Bermuda today is modulated by the nearby presence of the Gulf Stream current. However, iceberg scours in the Florida Strait and the presence of ice-rafted debris in Bermuda Rise sediments indicate that, during the last deglaciation, icebergs discharged from the Laurentide Ice Sheet traveled as far south as subtropical latitudes. We present evidence that an event of similar magnitude affected the subtropics during the Last Interglacial, potentially due to melting of the Greenland Ice Sheet. Using the clumped isotope paleothermometer, we found temperatures ~10°C colder and seawater $\delta^{18}O$ values ~2‰ lower than modern in Last Interglacial *Cittarium pica* shells from Grape Bay, Bermuda. In contrast, Last Interglacial shells from Rocky Bay, Bermuda, record temperatures only slightly colder and seawater $\delta^{18}O$ values similar to modern, likely representing more typical Last Interglacial conditions in Bermuda outside of a meltwater event. The significantly colder ocean temperatures observed in Grape Bay samples illustrate the extreme sensitivity of Bermudian climate to broad-scale ocean circulation changes. They indicate routine meltwater transport in the North Atlantic to near-equatorial latitudes, which would likely have resulted in disruption of the Atlantic Meridional Overturning Circulation. These data demonstrate that future melting of the Greenland Ice Sheet, a potential source of the Last Interglacial meltwater event, could have dramatic climate effects outside of the high latitudes.

1. Introduction

1.1. Paleoclimate of Bermuda

The modern warm climate in Bermuda is derived from the warm Gulf Stream current mixing with the relatively stagnant Sargasso Sea [*Steinberg et al.*, 2001]. The Gulf Stream follows the shelf-slope break along the U.S. East Coast until it reaches Cape Hatteras, where it veers eastward and crosses the North Atlantic along a northeast track until reaching Europe. As a result of the influence of the Gulf Stream, Bermuda has the northernmost warm water coral reefs in the Atlantic. The current likely also contributes to a warmer climate in Europe than would otherwise occur at that latitude [*Palter*, 2015].

There is evidence that the Gulf Stream has not always warmed Bermuda's climate. During the last glacial interval, ice-rafted debris was deposited in the Sargasso Sea [*Keigwin and Boyle*, 1999], coinciding with intervals of iceberg discharge from the Laurentide Ice Sheet known as Heinrich events [*Hemming*, 2004]. In Bermuda Rise sediments, diatom blooms confirm that meltwater traveled as far south as Bermuda during Heinrich events [*Gil et al.*, 2009]. Sea floor scours left by grounded icebergs are seen as far south as the Straits of Florida (25°N [*Hill and Condron*, 2014; *Hill et al.*, 2008]) and have been correlated to Heinrich events [*Goff and Austin*, 2009] (Figure 1). Modeling studies confirm that with sufficient meltwater discharge, icebergs can survive to these southerly latitudes and would be accompanied by cool, fresh meltwater [*Hill and Condron*, 2014]. Heinrich events mainly occurred during the most recent glacial phase [*Hemming*, 2004], and Heinrich-like events occurred during every previous glacial interval back to the mid-Pleistocene transition [*Hodell et al.*, 2008]. Both the most recent and penultimate glacial terminations are marked by large ice discharge events as ice sheets began to melt (Heinrich events 1 and 11, respectively) [*Hemming*, 2004]. Outside of the glacial phase, mid-interglacial ice melt events, such as the melting of the Greenland Ice Sheet [*Dutton et al.*, 2015], may also have introduced meltwater into the North Atlantic in a similar fashion. It is therefore possible that meltwater reached Bermuda at many other points outside the above mentioned Heinrich events, but no clear evidence of this yet exists.

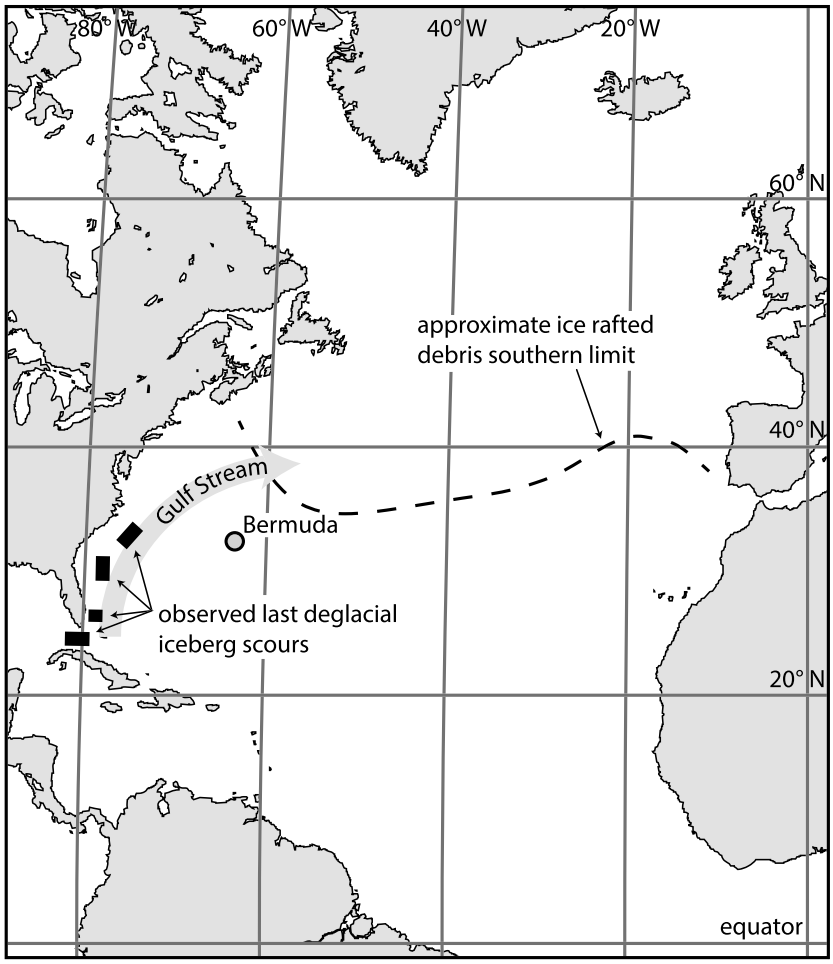

Figure 1. The North Atlantic Ocean, with key deglaciation features as described in the text. The ice-rafted debris limit includes Heinrich events 1–11 [*Ruddiman*, 1977; *Hemming*, 2004]. The last deglaciation iceberg scours are described by *Hill and Condron* [2014].

The Devonshire Marine Member of the Rocky Bay Formation of Bermuda been dated to marine isotope stage (MIS) 5e [*Muhs et al*., 2002], which is synonymous with the Last Interglacial interval. Based on faunal assemblages, it has been proposed that local climate was slightly warmer during the Last Interglacial [*Muhs et al*., 2002], but a virtual absence of emergent life position fossil corals on Bermuda during the interval [*Rowe and Bristow*, 2015] may reflect cooler temperatures relative to today. Carbonate-clumped isotope analysis of fossil shells in Rocky Bay Formation deposits can reveal quantitative information about temperature and the isotopic composition of seawater ($\delta^{18}O_w$) during Last Interglacial sea level rise intervals.

1.2. Application of Clumped Isotopes to Fossil Shells

The carbonate clumped isotope thermometer is useful for paleoclimatic and paleooceanographic applications because it enables direct measurement of formation temperature without the $\delta^{18}O_w$ assumptions required for conventional $\delta^{18}O$ thermometry [*Eiler*, 2011]. First empirically validated by *Ghosh et al*. [2006], the technique is based on the tendency of the rare and heavy isotopes (^{13}C and ^{18}O) to be preferentially bonded ("clumped") within a carbonate molecule at lower temperatures. The excess of isotopologues containing both heavy isotopes, relative to a random distribution of all isotopes among all isotopologues, is measured as a Δ_{47} value [*Schauble et al*., 2006; *Ghosh et al*., 2006]. Under most scenarios, Δ_{47} is dependent on temperature of formation alone [*Schauble et al*., 2006]. Because the clumped isotope technique enables simultaneous measurement of Δ_{47} and carbonate $\delta^{18}O$, the oxygen isotopic composition can then be calculated for the water in which the carbonate formed ($\delta^{18}O_w$ value).

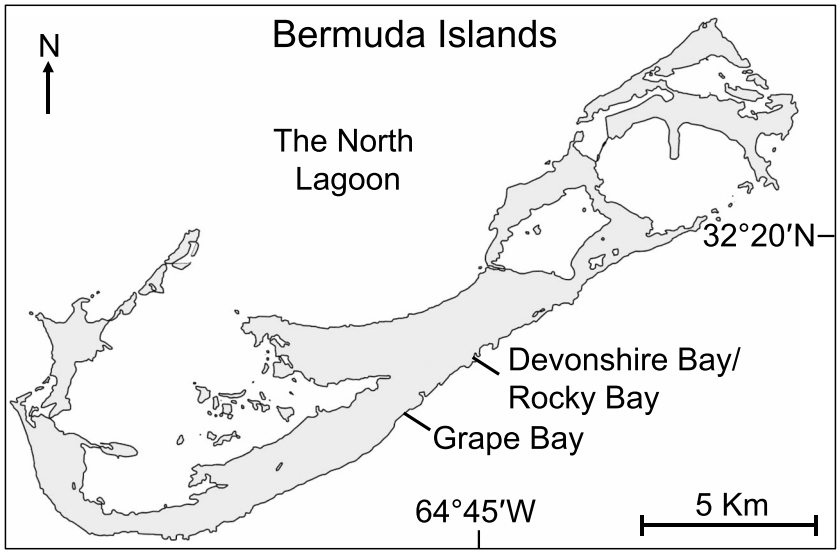

Figure 2. Map of Bermuda indicating sampling locations.

The clumped isotope technique still faces several challenges, including solid-state reordering of the carbonate lattice [*Passey and Henkes*, 2012] as well as increased susceptibility to diagenesis under burial conditions, relative to $\delta^{18}O$ [*Winkelstern and Lohmann*, 2016]. Furthermore, the multitude of published calibrations of the Δ_{47}-temperature relationship reveals significant intralaboratory disagreement [e.g., *Ghosh et al*., 2006; *Dennis and Schrag*, 2010; *Zaarur et al*., 2013; *Fernandez et al*., 2014; *Defliese et al*., 2015]. The effects of burial diagenesis, however, are not a concern for surficial deposits on Bermuda, and calibration uncertainty can be reduced by using a temperature calibration developed in the same laboratory in which analyses of unknown samples are carried out. The clumped isotope paleothermometer can be confidently applied to mollusk shells in particular because no mollusk-specific vital effects have been clearly observed in any species studied to date [*Eagle et al*., 2013; *Henkes et al*., 2013], with the possible exception of ammonites [*Dennis et al*., 2013].

Clumped isotopes can also enhance well-established isotope sclerochronology techniques. The study of fine-scale isotopic variation (often $\delta^{18}O$ and $\delta^{13}C$) across shell ontogeny is a powerful tool for obtaining paleoenvironmental records at subannual or better resolution [e.g., *Jones et al*., 1986; *Schöne and Surge*, 2012]. A similarly high-resolution sampling approach is generally not feasible for clumped isotope analysis, as required measurement time ($>$2 h) and sample size (typically $>$4 mg per replicate) are vastly increased relative to conventional stable isotope analysis. However, outside of estuarine and polar regions, interannual shifts in seawater $\delta^{18}O_w$ at a given location are typically well below 1‰ [*Stevenson et al*., 2015]. A single clumped isotope-derived $\delta^{18}O_w$ value from a marine shell can therefore reasonably be used to calculate a high-resolution seasonal sea surface temperature (SST) record from sclerochronological $\delta^{18}O$ data.

Here we present new $\delta^{18}O_w$ and high-resolution SST data from Last Interglacial shells from Bermuda, derived using the clumped isotope paleothermometer and high-resolution $\delta^{18}O$ analyses. We verify the accuracy of our methodology by applying the same techniques to modern shells. We then compare our measured paleotemperature data to modern climate, previous estimates of Last Interglacial temperature, and expected conditions during rapid meltwater input into the North Atlantic.

2. Methods

2.1. Fossil Selection and Geologic Context

We sampled a total of eight *Cittarium pica* gastropod fossils from two localities in Bermuda: Grape Bay and Rocky Bay (Figure 2). Fossils come from the Devonshire Marine Member of the Rocky Bay Formation. The Devonshire Marine Member is made up of transgressive lag deposits that represent initial flooding during

a sea level highstand interval [*Rowe and Bristow*, 2015]. The base of the unit is now roughly 2 m above sea level at both localities. *C. pica* is abundant in the deposits studied, and all fossil samples were taken from <1 m of sedimentary section within the upper portion of the <2 m thick Devonshire Marine Member. The two localities are considered coeval by stratigraphic interpretation [*Vacher and Hearty*, 1989] and have both been independently dated to the Last Interglacial [*Hearty et al*., 1992; *Muhs et al*., 2002].

C. pica is known in Bermuda only during interglacial intervals, including the current one [*Olson and Hearty*, 2013]. This species is thought to recolonize the island at the very onset of interglacial intervals [*Olson and Hearty*, 2013]. *C. pica* usually lives at the surface and does not live deeper than 7 m in the water column [*Welch*, 2010], meaning that temperature information recorded in its shell carbonate represents true SST. In addition to eight fossil shells, two live *C. pica* shells were collected at the same time under permit near Cooper's Island, Bermuda, in 2011. These modern specimens were measured alongside fossil shells to ensure that our combined clumped isotope and $\delta^{18}O$ sclerochronology approach accurately reproduced observed modern SST ranges and $\delta^{18}O_w$ values.

2.2. Geochemical Methodology

Carbonate samples were measured for their stable and clumped isotopic composition at the University of Michigan Stable Isotope Laboratory. For clumped isotope analysis, ~25 mg samples were chipped off the terminal edge of each shell and powdered via mortar and pestle. This sampling method targets the youngest material from each shell, which represents the final weeks to months of growth. Subsequently, shells were cut to reveal a cross section of growth and ~30 submonthly resolution carbonate samples of ~0.2 mg each were collected along the growth axis using a Micromill computerized drill. These microsamples were analyzed for conventional stable isotopes ($\delta^{18}O$ and $\delta^{13}C$). Because some shells are very thin near their terminal edge, microsampling began ~1 cm from the edge. The youngest conventional stable isotope measurements therefore reflect slightly earlier conditions than the clumped isotope measurements.

For conventional stable isotope analysis, samples were analyzed on a Kiel IV automated preparation device connected to a Thermo Scientific MAT 253 isotope ratio mass spectrometer. The $\delta^{18}O$ and $\delta^{13}C$ values were normalized relative to coanalyzed international standards (National Bureau of Standards (NBS) 19 and NBS 18). Analytical precision was better than 0.1‰.

For clumped isotope analysis, CO_2 was extracted from each powdered carbonate sample using an off-line sample preparation procedure (for further details, see *Defliese et al*. [2015]). Each aliquot was reacted individually in anhydrous phosphoric acid in a common acid bath at 75°C for 20 min (until completion). Residual water vapor was removed from resultant CO_2 via cryogenic procedures under vacuum conditions. To eliminate hydrocarbon and halocarbon contaminants, gas was passed through Porapak™ resin held at −30°C for 15 min (shells RB1, RB3, and RB6) or at −15°C for 10 min (all other shells). CO_2 was then measured on a Thermo Scientific MAT 253 stable isotope ratio mass spectrometer configured for Δ_{47} analysis, where masses 44 through 49 were measured for 60–80 cycles per replicate. CO_2 samples heated to 1000°C and CO_2 equilibrated with water at 25°C were used to monitor machine conditions and establish the absolute reference frame [*Dennis et al*., 2011]. Final clumped isotope values incorporate an acid fractionation factor of 0.067‰ for a 75°C reaction temperature [*Defliese et al*., 2015]. The $\delta^{18}O$ and $\delta^{13}C$ values acquired during clumped isotope analysis under the colder Porapak configuration (<−30°C) were corrected for fractionations introduced by the Porapak trap according to *Petersen et al*. [2016a].

Temperatures were calculated from Δ_{47} values using the ≥75°C acid compiled calibration of *Defliese et al*. [2015]. This calibration is based on compiled data from several calibration studies, including data measured on the same apparatus as the samples in this study, thereby reducing the impact of any unaccounted for laboratory-specific effects. Also, reassuringly, the *Defliese et al*. [2015] Δ_{47}-temperature relationship is similar to those found in the mollusk-specific studies of *Henkes et al*. [2013] and *Eagle et al*. [2013].

The $\delta^{18}O$ values of bulk samples acquired during clumped isotope analysis were corrected for acid fractionation via *Kim et al*. [2007b]. The isotopic composition of the water from which the shells precipitated was calculated using the *Kim et al*. [2007a] aragonite-water fractionation factor, which is very similar to the

mollusk-specific fractionation factor of *Grossman and Ku* [1986]. All carbonate $\delta^{18}O$ and $\delta^{13}C$ values are reported relative to the Vienna Peedee belemnite standard, and all $\delta^{18}O_w$ values are reported relative to the Vienna standard mean ocean water standard.

We created seasonal SST records for all shells by combining each clumped isotope-derived $\delta^{18}O_w$ value with the corresponding high-resolution shell $\delta^{18}O$ measurements via the *Kim et al.* [2007a] fractionation factor. This method assumed that $\delta^{18}O_w$ was constant throughout the time interval sampled at high resolution (1 to 3 years), which is discussed below.

2.3. Diagenesis and Local Freshwater Input

We assessed diagenetic alteration of fossil material through X-ray diffraction (XRD), inspection under microscope, and isotopic analysis of fossils and surrounding material. XRD analyses were conducted on a Rigaku Ultima IV diffractometer at the University of Michigan, with detection limits of 5% or better. We found excellent preservation for all samples, including 100% aragonitic composition via XRD, visible shell microstructure, and consistent intra-locality stable isotope values that contrast with surrounding bulk rock material by multiple per mil (Table 1). Co-occurring Pleistocene diagenetic cements record clumped isotope-derived $\delta^{18}O_w$ values distinct and lower than fossil shells, indicating that these shells were not reset or recrystallized during the diagenetic events that formed those cements [*Defliese and Lohmann*, 2016]. Clear seasonality in high-resolution SST time series and consistent intra-locality reconstructed $\delta^{18}O_w$ values and SSTs also suggest preservation of original isotopic composition (Figures 3 and 4).

In a coastal setting it is prudent to consider the possibility of seasonal freshwater delivery causing temporal variations in $\delta^{18}O_w$ values. Because of Bermuda's small size, however, no surface freshwater reservoir currently exists [*Vacher*, 1978]. During the Last Interglacial interval, Bermuda's size and hydrogeology were similar to today [*Defliese and Lohmann*, 2016], and it is highly unlikely that local freshwater inputs were capable of significantly lowering local $\delta^{18}O_w$ or salinity. Modern measured seawater $\delta^{18}O_w$ in the surrounding area varies from +1.01 to +1.36‰ [*Schmidt et al.*, 1999]. This small range supports our assumption that subannual $\delta^{18}O_w$ variability was minor in the past and was not strongly influenced by local freshwater input. Lower Last Interglacial seawater $\delta^{18}O_w$ values calculated from clumped isotope measurements are therefore most likely the result of large-scale changes in the $\delta^{18}O_w$ composition of North Atlantic surface waters.

3. Results

3.1. Modern Shells

We found good correspondence between Δ_{47}-derived temperatures for the two modern shells and modern SSTs concurrently measured by NOAA buoys nearby [*Hervey et al.*, 2013]. Carbonate samples for clumped isotope analysis were taken from the last ~5 mm of each shell, which based on time of collection, should represent the summer months. The two modern shells record temperatures of 30.0 ± 1.0°C and 27.7 ± 1.3°C (Table 1 and Figure 3) compared to the modern mean summertime temperature of ~28°C and maximum temperature of ~31°C [*Hervey et al.*, 2013]. The $\delta^{18}O_w$ values for the two modern shells were $+1.7 \pm 0.3$‰ and $+1.5 \pm 0.4$‰, in close agreement with each other, and slightly higher than the local average seawater $\delta^{18}O_w$ value of +1.1‰ reported in the Global Seawater Oxygen-18 Database [*Schmidt et al.*, 1999] (Figure 3). These modern $\delta^{18}O_w$ measurements were not conducted at the same time or at the exact location where the modern shells were collected, and so would be expected to differ slightly from the shell's environment [*Schmidt et al.*, 1999]. Taken together, these data confirm that clumped isotope measurements of *C. pica* can accurately represent local climate conditions.

More critically, we found excellent agreement between the observed seasonal range of modern SSTs and reconstructed SST time series from high-resolution sampling of the modern shells (Figure 4, top). High-resolution $\delta^{18}O$ data, converted to temperature using the mean $\delta^{18}O_w$ value from each shell, match closely with the magnitude and range of the seasonal cycle in temperature today in Bermuda (Figure 4). Reconstructed temperatures from modern shells vary from 19 to 30°C, giving a total range of 11°C. Modern temperatures when these shells were growing (2009 to 2011) range from 16 to 31°C, in close agreement with reconstructed temperatures from live-collected shells.

Table 1. Data From Replicate Clumped Isotope Analyses for Each Shell, Along With the Bulk Rock From Which Rocky Bay Fossil Shells Were Sampled[a]

Shell	$\delta^{13}C$ (‰ VPDB)	Mean $\delta^{13}C$	$\delta^{18}O$ (‰ VPDB)	Mean $\delta^{18}O$	Δ^{47} (‰ ARF)	Mean Δ^{47}	Mean Δ^{47}°C	Mean $\delta^{18}O_w$ (‰ VSMOW)
Modern1	−0.85	−0.74 ± 0.06	−0.82	−0.87 ± 0.03	0.700	0.682 ± 0.005	30.0° ± 1.0°	+1.7 ± 0.3
	−0.75		−0.74		0.691			
	−0.79		−0.86		0.669			
	−0.61		−0.95		0.689			
	−0.54		−0.96		0.670			
	−0.93		−0.93		0.675			
Modern2	+0.06	+0.08 ± 0.17	−0.89	−0.67 ± 0.11	0.675	0.689 ± 0.006	27.7° ± 1.3°	+1.5 ± 0.4
	+0.56		−0.28		0.717			
	−0.69		−0.90		0.693			
	+0.13		−0.66		0.670			
	−0.09		−0.91		0.692			
	+0.53		−0.31		0.687			
GB1	+2.05	+2.02 ± 0.02	−0.27	−0.24 ± 0.04	0.739	0.719 ± 0.010	17.3° ± 2.1°	−0.3 ± 0.7
	+2.05		−0.14		0.710			
	+2.03		−0.35		0.738			
	+1.95		−0.22		0.690			
GB3	+2.32	+2.35 ± 0.02	−0.46	−0.41 ± 0.02	0.718	0.726 ± 0.005	15.0° ± 1.0°	−0.9 ± 0.3
	+2.43		−0.36		0.723			
	+2.33		−0.42		0.718			
	+2.33		−0.41		0.743			
GB5	+3.32	+3.32 ± 0.01	−0.43	−0.43 ± 0.02	0.747	0.728 ± 0.011	14.5° ± 2.2°	−1.0 ± 0.8
	+3.35		−0.45		0.752			
	+3.29		−0.46		0.699			
	+3.35		−0.38		0.715			
GB7	+2.23	+2.25 ± 0.01	+0.20	+0.29 ± 0.05	0.712	0.721 ± 0.005	16.4° ± 1.1°	+0.1 ± 0.3
	+2.26		+0.24		0.734			
	+2.24		+0.26		0.710			
	+2.26		+0.46		0.729			
RB1	+2.49	+2.43 ± 0.08	−0.06	−0.03 ± 0.09	0.692	0.698 ± 0.007	24.3° ± 1.4°	+1.4 ± 0.5
	+2.47		+0.27		0.691			
	+2.17		−0.21		0.722			
	+2.60		−0.10		0.689			
RB3	+2.46	+2.41 ± 0.04	+0.41	+0.46 ± 0.02	0.706	0.696 ± 0.003	24.9° ± 0.7°	+2.1 ± 0.2
	+2.29		+0.50		0.688			
	+2.49		+0.46		0.696			
	+2.42		+0.47		0.696			
RB6	+2.98	+2.96 ± 0.06	+0.58	+0.49 ± 0.04	0.729	0.715 ± 0.012	18.8° ± 2.5°	+0.8 ± 0.8
	+3.02		+0.37		0.755			
	+3.07		+0.62		0.717			
	+3.06		+0.50		0.697			
	+2.69		+0.38		0.677			
RB48	+3.09	+3.01 ± 0.04	+0.33	+0.28 ± 0.04	0.701	0.707 ± 0.009	21.3° ± 1.8°	+1.1 ± 0.6
	+3.11		+0.32		0.738			
	+2.99		+0.31		0.711			
	+2.95		+0.14		0.680			
	+2.82		+0.18		0.729			
	+3.09		+0.39		0.685			
Bulk Rock	−3.89	−4.07 ± 0.09	−2.27	−2.92 ± 0.36	0.693	0.721 ± 0.013	16.3° ± 2.6°	−2.9 ± 1.2
	−4.27		−2.75		0.723			
	−4.05		−3.76		0.747			

[a]All errors are 1 standard error of the mean. Water $\delta^{18}O$ values ($\delta^{18}O_w$) are calculated using the aragonite-water fractionation factor of *Kim et al.* [2007a, 2007b]. Clumped isotope (Δ_{47}) values are reported in the absolute reference frame (ARF) of *Dennis et al.* [2011], and Δ_{47}-derived temperatures are calculated via the *Defliese et al.* [2015] ≥75°C acid calibration.

3.2. Fossil Shells

All analyzed fossil shells record significantly colder temperatures than modern shells, with high-resolution calculated fossil SSTs ranging between 8 and 27°C, compared to the modern range of 16 to 31°C (Figures 3 and 4). The average difference between highest and lowest SSTs within each shell (seasonality) is smaller for fossil shells (~8°C) than modern shells (~11°C). However, the difference between the

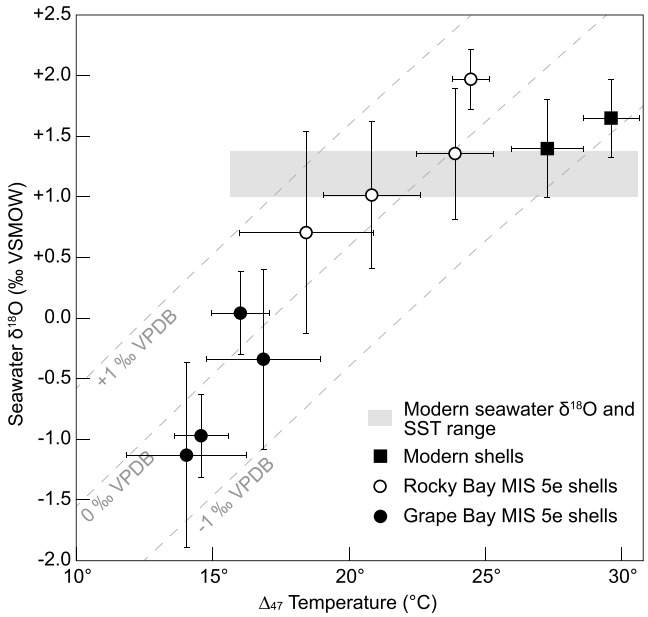

Figure 3. Clumped isotope temperatures plotted against calculated water $\delta^{18}O$ (‰, VSMOW) for each shell. Dashed lines indicate the carbonate $\delta^{18}O$ (‰, VPDB) values for reference. The modern range of sea surface temperatures (SSTs) is from 2009 to 2011 NOAA buoy data. The range of modern seawater $\delta^{18}O$ values is from the Global Seawater Oxygen-18 Database [*Schmidt et al.*, 1999] (http://data.giss.nasa.gov/o18data/).

highest and lowest SST values recorded among all shells in the modern (~11°C), Grape Bay (~12°C), and Rocky Bay shell sets (~11°C) is essentially constant. This indicates similar multiannual variability (Figure 4).

Shells from Rocky Bay and Grape Bay populate two distinct temperature ranges. Temperatures in Rocky Bay are 16 to 27°C, ~2°C lower than modern on average, whereas temperatures recorded by Grape Bay shells are 8 to 20°C, averaging ~10°C colder than modern (Figure 4). This is surprising, given the fact that the carbonate $\delta^{18}O$ values are very similar between Grape Bay, Rocky Bay, and modern shells (Figure 3). Under normal assumptions a constant $\delta^{18}O_w$ value representative of interglacial conditions, such as 0‰, would be used to calculate mean temperature from shell $\delta^{18}O$. This method would have resulted in nearly identical temperatures for Grape Bay and Rocky Bay (as well as modern) shells. The clumped isotope technique instead allows for the direct calculation of $\delta^{18}O_w$ values, and measurements show that $\delta^{18}O_w$ values are distinct between the two localities as well, with Rocky Bay recording $\delta^{18}O_w$ values of +0.5 to +2.0‰ and Grape Bay recording lower $\delta^{18}O_w$ values of -1 to 0‰ (Figure 3).

4. Discussion

4.1. Temporal Disparity Between Rocky Bay and Grape Bay Deposits

The Rocky Bay and Grape Bay shells fall into two separate regimes in temperature and $\delta^{18}O_w$. The difference is ~7°C and ~2‰, respectively, between the two localities. These differences are much too great to be explained by spatial variability, especially considering that the two sites are only ~2 km apart (Figure 2). We suggest instead that these two lag deposits, despite being assigned to the same formation member, are in fact temporally distinct.

The Devonshire Marine Member is made up of sporadic lag deposits that are correlated in part based on their relationship to underlying deposits of the Belmont Formation that represent MIS 7 [*Rowe et al.*, 2014]. The Grape Bay and Rocky Bay outcrops of the Devonshire Marine Member cannot be laterally traced between the two localities to confirm that they are the same deposit [*Vacher et al.*, 1995]. The Devonshire Marine deposits in both localities have been dated to MIS 5e, but the dating is not precise enough to determine the relative age of the two deposits within the interglacial interval. Grape Bay corals give U-Th ages of 113–125 ka [*Muhs et al.*, 2002], whereas Rocky Bay corals give a U-Th age of 125 ± 4 ka [*Harmon et al.*, 1983]. Combining samples of the Devonshire Marine Member from multiple locations (including those not

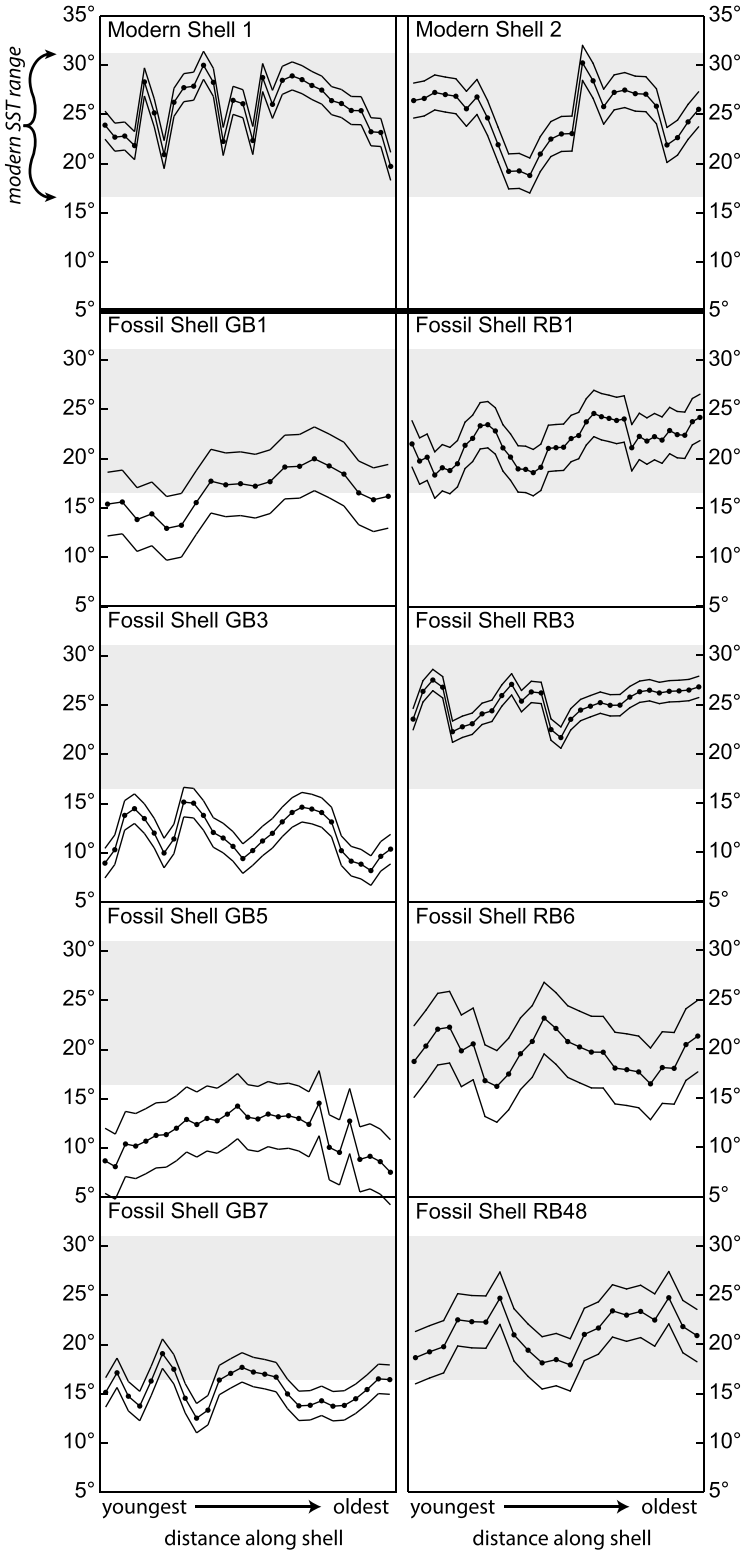

Figure 4. SST time series for each shell, calculated from aragonite $\delta^{18}O$ measurements along each shell's growth axis as well as clumped isotope-derived water $\delta^{18}O$ values from Figure 3. The distance between measurements (*x* axis) varies and depends on shell size, with shell death toward the left. The leftmost measurements here were taken within ~1 cm of each terminal shell edge but represent slightly older shell material than that sampled for clumped isotopes. Black lines indicate the SST error based on 1 standard error for calculated water $\delta^{18}O$. Shaded regions indicate the 2009–2011 SST range in Bermuda, the time during which modern shells were growing.

sampled here), individual U-Th dates range from 113 ± 0.9 ka at the youngest [*Muhs et al*., 2002] to 134 ± 8 ka at the oldest [*Harmon et al*., 1983].

There is some stratigraphic indication that MIS 5 units in Bermuda are made up of multiple deposits. *Vollbrecht* [1990] found two discernable sequences for MIS 5 based on seismic data that were spatially variable, with an irregular contact, but locally indistinguishable. Composite stratigraphy combining aminostratigraphy and allostratigraphy breaks the Rocky Bay Formation (which includes the Devonshire Marine Member) into two sequences (R1 and R2), potentially correlated to 5e [*Vacher et al*., 1995]. *Hearty and Kindler* [1995] suggested an early 5e and late 5e sea level highstand, as well as a later 5a highstand. Amino acid racemization dating found three distinct MIS 5 groupings [*Harmon et al*., 1983; *Hearty et al*., 1992]. U-Th dated corals from Spencer's Point, later designated as equivalent to the Devonshire Formation [*Hearty and Olson*, 2010], also showed three distinct groupings of ages between 134 and 83 ka, with the latest likely representing MIS 5a [*Harmon et al*., 1983].

It is therefore plausible that the Grape Bay and Rocky Bay lag deposits, which must have been laid down during periods of sea level rise, are temporally distinct. The combination of stratigraphic data with the divergent paleooceanographic conditions we observe makes it clear that separate paleoclimatic interpretations are required for each site. Whether these deposits represent separate Last Interglacial transgressions or simply different phases of a single transgression, however, cannot be conclusively established. The timing and cause of sea level rise are discussed below.

4.2. Grape Bay Deposits: Climate Effects of a Meltwater Pulse

Modeling suggests that meltwater discharged from Hudson Bay during deglacial ice sheet collapse, and produced by continued melting of icebergs (mimicking Heinrich event 1), could reduce salinities in the Sargasso Sea by as much as 6 practical salinity unit (psu) [*Hill and Condron*, 2014]. We propose that the Grape Bay shells are recording an influx of meltwater into the North Atlantic of a similar magnitude during the Last Interglacial.

Critically, Grape Bay fossils record $\delta^{18}O_w$ values significantly lower than modern and Rocky Bay samples. The Grape Bay $\delta^{18}O_w$ values are on average ~2‰ below the modern seawater values for Bermuda. Based on observed correlations between $\delta^{18}O_w$ and salinity in the modern surface ocean, a 2‰ reduction in $\delta^{18}O_w$ corresponds to a salinity decrease of ~4 to ~7 psu [*Broecker*, 1989], similar to the modeled salinity decrease for a Termination I meltwater event [*Hill and Condron*, 2014]. This estimate varies depending on the isotopic composition of the freshwater causing the salinity reduction, but nevertheless, the observed negative $\delta^{18}O_w$ values are consistent with a meltwater pulse reaching Bermuda.

Grape Bay shells also record temperatures 5–10°C colder than modern. This could be the result of cool, fresh meltwater delivery but could also be associated with related large-scale circulation changes. The input of large amounts of freshwater into the North Atlantic is known to affect the Atlantic Meridional Overturning Circulation and would also impact Gulf Stream strength and position [*Alley*, 2007]. The magnitude of cooling observed in the Grape Bay shells is similar to that seen in models of deglacial meltwater input, where meltwaters have freshened the subtropical gyre [*Hill and Condron*, 2014].

The duration of the meltwater delivery event is not well constrained because the sampled *C. pica* organisms could have lived at the same time or hundreds of years apart. A transgressive lag deposit inherently concentrates and sorts fossil material, and thus, relative age of shells within a single horizon cannot be determined from stratigraphy [*Hwang and Heller*, 2002]. At a minimum the cold conditions lingered for several years, as all shells record consistent conditions over their 1–4 year life spans. The cooler climate conditions probably lasted longer than a few years, given the low likelihood of all four measured shells living in the exact same 4 year interval. The timing of this event within the Last Interglacial is discussed below.

The cold SSTs we observe have interesting implications for faunal analog reconstructions. Nowhere in the world today are *C. pica* found inhabiting waters as cold as those recorded in the Grape Bay fossils. Today, *C. pica* only live in locations with mean annual temperatures above 20°C [*Olson and Hearty*, 2013]. Based on the isotope sclerochonologies, summer temperatures recorded by Grape Bay shells never exceed ~20°C (Figure 4). These temperatures are comparable to modern winter temperatures in Bermuda. The Last Interglacial winter SSTs recorded by these shells of 7 to 14°C are almost never observed in Bermuda today [*Hervey et al*., 2013]. This shows definitively that the modern accepted thermal tolerance of *C. pica* does

not apply in all paleoclimate cases, and assessments of past warm temperatures based on the presence of *C. pica* may be incorrect [*Muhs et al*., 2002]. In addition to mollusks, the reefal corals around the island today could not survive in the conditions described by Grape Bay shells [*Kleypas et al*., 1999]. This is consistent with the lack of life-position corals found in MIS 5e sediments on Bermuda [*Rowe and Bristow*, 2015].

4.3. Rocky Bay Deposits: Representative of Interglacial Conditions

Relative to the unexpectedly low seawater $\delta^{18}O_w$ values and cold SSTs recorded by Grape Bay shells, Rocky Bay shells record conditions much more similar to modern. Rocky Bay SSTs significantly overlap the range of modern conditions, although average SSTs are ~2°C colder than today (Figure 4). Rocky Bay temperatures are also in good agreement with MIS 5e SST estimates of 23 to 26°C based on foraminiferal assemblages within core MD95-2036 (34°N, 58°W), ~700 km NE of Bermuda [*Cortijo et al*., 1999]. The $\delta^{18}O_w$ values recorded by Rocky Bay shells (on average ~1.4‰) are similar to the modern mean of +1.1‰ and again in agreement with data from MD95-2036. Seawater $\delta^{18}O$ values of +0.5 to +1.5‰ were reconstructed for MD95-2036 by combining foraminiferal $\delta^{18}O$ measurements with SSTs reconstructed from the modern analog technique [*Cortijo et al*., 1999].

Taken together, this suggests that Last Interglacial conditions in Bermuda were broadly similar to today in seawater $\delta^{18}O_w$ and seasonality but slightly colder on average. Other western North Atlantic proxy data suggest that the region was broadly similar to or slightly cooler than modern [*Rahmstorf*, 2002]. Slightly cooler Last Interglacial conditions are consistent with the larger pattern of warmer poles and cooler tropics observed in compiled MIS 5e SST proxy data [*Turney and Jones*, 2010; *Capron et al*., 2014]. This pattern suggests that the observed cooling could be due to shifts in oceanic circulation, such as changing Gulf Stream strength and/or position.

Interestingly, the reconstructed SST time series from Rocky Bay shells indicate that most of the observed Last Interglacial cooling is due to colder than modern summer temperatures (Figure 4). Maximum recorded SSTs for Rocky Bay shells never approach modern maximum SST, while minimum SSTs are roughly the same as today (Figure 4). This could perhaps reflect a more energetic Gulf Stream that would foster enhanced surface ocean mixing via more intrusions of cold-core rings into the Sargasso Sea. This could possibly inhibit the enhanced summertime heating of relatively stagnant waters that occurs today, relative to eastern North Atlantic waters at the same latitude [*Hogg and Johns*, 1995; *Locarnini et al*., 2013]. Subannual resolution SST data covering more of the North Atlantic would be needed to evaluate this hypothesis.

4.4. Last Interglacial Sea Level in Bermuda and Meltwater Sourcing

Despite evidence for minor tectonic instability [*Rowe et al*., 2014], it is highly likely that Rocky Bay and Grape Bay deposits (currently ~2 m above sea level) were laid down when local, relative sea level was higher than modern. During the Last Interglacial, global, eustatic sea level was above modern from ~129 to ~116 ka [*Stirling et al*., 1998; *Masson-Delmotte et al*., 2013]. Relative sea level rise in Bermuda is predicted to lag behind eustatic sea level rise by a few thousand years because of isostatic effects [*Dutton and Lambeck*, 2012], suggesting that sea levels in Bermuda could have only exceeded modern levels around ~125–127 ka at the earliest.

One potential source for the meltwater pulse indicated by Grape Bay shells would be deglacial ice discharge from a collapsing Laurentide Ice Sheet. A meltwater signal associated with Heinrich event 11 (negative shifts in $\delta^{18}O$ water and the presence of ice-rafted debris) has been observed in multiple North Atlantic sediment cores [e.g., *Cortijo et al*., 1999; *Hemming*, 2004], and the reduction in temperature and $\delta^{18}O_w$ observed in the Grape Bay shells is similar in magnitude to modeled SST and salinity reductions for Laurentide Ice Sheet discharge [*Hill and Condron*, 2014].

However, Heinrich event 11 (dated to 135 ± 1 to 130 ± 2 ka [*Haüselmann et al*., 2015; *Marino et al*., 2015]) occurs too early to be recorded in the Rocky Bay Formation deposits, when sea levels were still well below modern. Radiometric dates from Grape Bay and Rocky Bay coral specimens indicate that these units are not older than 125 ± 4 ka, and deposits in Grape Bay specifically are not older than 126.3 ka, including reported error [*Muhs et al*., 2002] (Figure 5). Based on these dates and the estimated timing of relative sea level surpassing modern levels in Bermuda, Grape Bay and Rocky Bay deposits were most likely laid down later in the interglacial, a result of a secondary pulse of MIS 5e sea level rise.

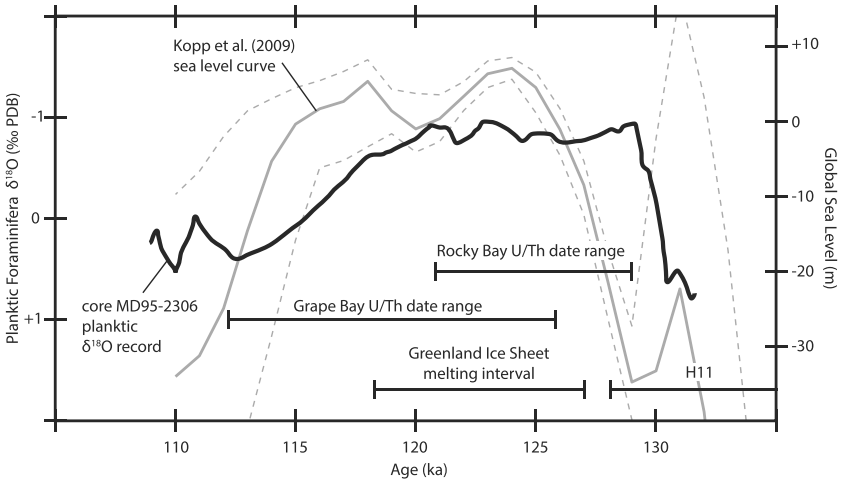

Figure 5. The age range of Grape Bay and Rocky Bay deposits (via *Muhs et al.* [2002] and *Harmon et al.* [1983]) is placed with other Last Interglacial changes for context. The global sea level curve of *Kopp et al.* [2009] is plotted with the smoothed planktonic foraminiferal $\delta^{18}O$ record of *Adkins et al.* [1997] from Bermuda Rise core MD95-2306 (~700 km northeast of Bermuda). The solid grey line indicates the median sea level projection, with dashed grey lines indicating 16th and 84th percentiles. The interval for Greenland Ice Sheet melting is from *Colville et al.* [2011], and the interval for H11 (Heinrich event 11) is from *Haüselmann et al.* [2015].

During the interval when eustatic sea level exceeded modern levels (~129 to ~116 ka), reconstructions disagree on whether stable MIS 5e global mean sea level abruptly increased late in the interglacial [*Blanchon et al.*, 2009; *O'Leary et al.*, 2013] or if multiple eustatic sea level oscillations occurred [*Rohling et al.*, 2008; *Thomson et al.*, 2011]. In addition to Heinrich event 11, at least two pulses of global, eustatic, sea level rise have been identified during the Last Interglacial in a Bayesian composite analysis [*Kopp et al.*, 2009] (Figure 5). The first corresponds with the penultimate deglaciation via melting of continental ice sheets (Termination II), and the second occurs in the middle of the interglacial interval around 118 ka [*Kopp et al.*, 2009]. This second sea level rise event likely included contributions from both the Greenland and West Antarctic Ice Sheets [*Dutton et al.*, 2015]. The southern portion of the Greenland Ice Sheet in particular underwent substantial melting between ~122 and ~119 ka [*Colville et al.*, 2011; *NEEM Community Members*, 2013]. Given the location of Bermuda in the North Atlantic and the time constraints on deposition, it is possible, and perhaps likely, that the meltwater pulse recorded by Grape Bay shells came from rapid melting of the Greenland Ice Sheet.

4.5. Utility of Clumped Isotope Thermometry

Despite recording very different temperatures and seawater $\delta^{18}O$ values, the Rocky Bay, Grape Bay, and modern shells record very similar carbonate $\delta^{18}O$ values. If typical assumptions of invariant $\delta^{18}O_w$ identical to today were used, the range in carbonate $\delta^{18}O$ recorded in all these shells (−0.87‰ to +0.49‰) would only explain a 5°C difference in temperature, much smaller than the observed range of 18°C between the coldest and warmest shells (GB5 versus Modern 1). From carbonate $\delta^{18}O$ alone, there was no indication of the wide range in seawater $\delta^{18}O_w$ values that were contained in the clumped isotope signal. This is because cooler temperatures coincided with depleted seawater $\delta^{18}O$ values during the meltwater event. Evidence for a meltwater event could only have been obtained from these shells using the independent temperature measurement provided by clumped isotope thermometry. Following several other studies [e.g., *Dennis et al.*, 2013; *Drury and John*, 2013; *Grauel et al.*, 2013; *Tripati et al.*, 2014; *Petersen and Schrag*, 2015; *Petersen et al.*, 2016b], these results emphasize the utility of clumped isotope thermometry for paleooceanographic applications.

5. Conclusions

Based on our limited sample set, the stable isotopes of Last Interglacial fossil material from Bermuda reveal large variations in SST and seawater $\delta^{18}O_w$ during the interval. Notably, the Grape Bay shell data are consistent with meltwater influx into the subtropics. This meltwater event almost certainly occurred late in the

interglacial, after sea level in Bermuda was high enough, with the most likely source being later melting of the Greenland Ice Sheet [e.g., *Schaefer et al*., 2016].

This possibility makes our results particularly relevant for the future of the North Atlantic. It appears that substantial and rapid melting occurred after thousands of years of sustained interglacial climate, when global ice volume was even smaller than today [*Dutton and Lambeck*, 2012]. In contrast to the relatively warm, modern-like conditions described by Rocky Bay shells, the shells from Grape Bay describe a cold subtropical ocean and likely severe weakening of North Atlantic Overturning Circulation. These conditions could be expected to recur given continued anthropogenic forcing and resultant melting of the Greenland Ice Sheet [*Hall et al*., 2013]. In Bermuda specifically, the cold SSTs we observed would have severe ecological effects, potentially including the demise of corals that today form protective reefs around the islands. Abrupt temperature change and disruption of ocean circulation driven by a meltwater pulse would certainly also have dramatic climate and ecological effects throughout the North Atlantic.

Acknowledgments
Reviews by Andrea Dutton and one anonymous reviewer greatly enhanced this manuscript. This work was supported NSF EAR grant 1123733 awarded to K.C.L. and by a Rackham Graduate School student grant awarded to I.Z.W. We thank Lora Wingate, Kyle Meyer, Clay Tabor, and Chris Poulsen for their discussion, and/or laboratory assistance and Colleen Long for the assistance in the field. We also thank Mark Outerbridge of the Bermuda Department of Conservation Services for facilitating the collection of modern shells. Data used to produce the results of this paper are attached as supporting information.

References

Adkins, J. F., E. A. Boyle, L. Keigwin, and E. Cortijo (1997), Variability of the North Atlantic thermohaline circulation during the Last Interglacial period, *Nature*, *390*, 154–156.

Alley, R. B. (2007), Wally was right: Predictive ability of the North Atlantic "conveyor belt" hypothesis for abrupt climate change, *Annu. Rev. Earth Planet. Sci.*, *35*, 241–272, doi:10.1146/annurev.earth.35.081006.131524.

Blanchon, P., A. Eisenhauer, J. Fietzke, and V. Liebetrau (2009), Rapid sea-level rise and back-stepping at the close of the Last Interglacial highstand, *Nature*, *458*, 881–884.

Broecker, W. S. (1989), The salinity contrast between the Atlantic and Pacific Oceans during glacial time, *Paleoceanography*, *4*, 207–212, doi:10.1029/PA004i002p00207.

Capron, E., A. Govin, E. J. Stone, V. Masson-Delmotte, S. Mulitza, B. Otto-Bliesner, T. L. Rasmussen, L. C. Sime, C. Waelbroeck, and E. W. Wolff (2014), Temporal and spatial structure of multi-millennial temperature changes at high latitudes during the Last Interglacial, *Quat. Sci. Rev.*, *103*, 116–133, doi:10.1016/j.quascirev.2014.08.018.

Colville, E. J., A. E. Carlson, B. L. Beard, R. G. Hatfield, J. S. Stoner, A. V. Reyes, and D. J. Ullman (2011), Sr-Nd-Pb isotope evidence for ice-sheet presence on southern Greenland during the Last Interglacial, *Science*, *333*, 620–623.

Cortijo, E., S. Lehman, L. Keigwin, M. Chapman, D. Paillard, and L. Labeyrie (1999), Changes in meridional temperature and salinity gradients in the North Atlantic Ocean (30°–72°N) during the Last Interglacial period, *Paleoceanography*, *14*, 23–33, doi:10.1029/1998PA900004.

Defliese, W. F., and K. C. Lohmann (2016), Evaluation of meteoric calcite cements as a proxy material for mass-47 clumped isotope thermometry, *Geochim. Cosmochim. Acta*, *173*, 126–141, doi:10.1016/j.gca.2015.10.022.

Defliese, W. F., M. T. Hren, and K. C. Lohmann (2015), Compositional and temperature effects of phosphoric acid fractionation on Δ47 analysis and implications for discrepant calibrations, *Chem. Geol.*, *396*, 51–60, doi:10.1016/j.chemgeo.2014.12.018.

Dennis, K. J., and D. P. Schrag (2010), Clumped isotope thermometry of carbonatites as an indicator of diagenetic alteration, *Geochim. Cosmochim. Acta*, *74*, 4110–4122.

Dennis, K. J., J. K. Cochran, N. H. Landman, and D. P. Schrag (2013), The climate of the Late Cretaceous: New insights from the application of othe carbonate clumped isotope thermometer to Western Interior Seaway macrofossil, *Earth Planet. Sci. Lett.*, *362*, 51–65.

Dennis, K. J., H. P. Affek, B. H. Passey, D. P. Schrag, and J. M. Eiler (2011), Defining an absolute reference frame for "clumped" isotope studies of CO_2, *Geochim. Cosmochim. Acta*, *75*, 7117–7131, doi:10.1016/j.gca.2011.09.025.

Drury, A. J., and C. M. John (2013), Exploring the potential of clumped isotope thermometry on coccolith-rich sediments as a sea surface temperature proxy, *Geochem. Geophys. Geosyst.*, 1525–2027, doi:10.1002/2016GC006459.

Dutton, A., and K. Lambeck (2012), Ice volume and sea level during the Last Interglacial, *Science*, *337*, 216–219.

Dutton, A., A. E. Carlson, A. J. Long, G. A. Milne, P. U. Clark, R. DeConto, B. P. Horton, S. Rahmstorf, and M. E. Raymo (2015), Sea level rise due to polar ice-sheet mass loss during past warm periods, *Science*, *349*(6244), 1–9, doi:10.1126/science.aaa4019.

Eagle, R. A., et al. (2013), The influence of temperature and seawater carbonate saturation state on ^{13}C-^{18}O bond ordering in bivalve mollusks, *Biogeosciences*, *10*, 4591–4606.

Eiler, J. M. (2011), Paleoclimate reconstruction using carbonate clumped isotope thermometry, *Quat. Sci. Rev.*, *30*, 3575–3588, doi:10.1016/j.quascirev.2011.09.001.

Fernandez, A., J. Tang, and B. E. Rosenheim (2014), Siderite "clumped" isotope thermometry: A new paleoclimate proxy for humid continental environments, *Geochim. Cosmochim. Acta*, *126*, 411–421.

Ghosh, P., J. Adkins, H. Affek, B. Balta, W. Guo, E. Schauble, D. Schrag, and J. Eiler (2006), ^{13}C-^{18}O bonds in carbonate minerals: A new kind of paleothermometer, *Geochim. Cosmochim. Acta*, *70*, 1439–1456.

Gil, I. M., L. D. Keigwin, and F. G. Abrantes (2009), Deglacial diaton productivity and surface ocean properties over the Bermuda Rise, northeast Sargasso Sea, *Paleoceanography*, *24*, PA4101, doi:10.1029/2008PA001729.

Goff, J. A., and J. A. Austin (2009), Seismic and bathymetric evidence for four different episodes of iceberg scouring on the New Jersey outer shelf: Possible correlation to Heinrich events, *Mar. Geol.*, *266*, 244–254.

Grauel, A.-L., T. W. Schmid, B. Hu, C. Bergami, L. Capotondi, L. Zhou, and S. M. Bernasconi (2013), Calibration and application of the "clumped isotope" thermometer to foraminifera for high-resolution climate reconstructions, *Geochim. Cosmochim. Acta*, *108*, 125–140.

Grossman, E. L., and T.-L. Ku (1986), Oxygen and carbon isotope fractionation in biogenic aragonite: Temperature effects, *Chem. Geol.*, *59*, 59–74, doi:10.1016/0168-9622(86)90057-6.

Hall, D. K., J. C. Comiso, N. E. DiGirolamo, C. A. Shuman, J. E. Box, and L. S. Koenig (2013), Variability in the surface temperature and melt extent of the Greenland ice sheet from MODIS, *Geophys. Res. Lett.*, *40*, 2114–2120, doi:10.1002/grl.50240.

Harmon, R. S., R. M. Mitterer, N. Kriausakul, L. S. Land, H. P. Schwarcz, P. Garrett, G. J. Larson, H. L. Vacher, and M. Rowe (1983), U-Series and amino-acid racemization geochronology of Bermuda: Implications for eustatic sea-level fluctuaton over the past 250,000 years, *Palaeogeogr. Palaeoclimatol. Palaeoecol.*, *44*, 41–70.

Haüselmann, A. D., D. Fleitmann, K. Cheng, D. Tabersky, D. Gunther, and R. L. Edwards (2015), Timing and nature of the penultimate deglaciation in a high alpine stalagmite from Switzerland, *Q. Sci. Rev.*, *126*, 264–275.
Hearty, P. J., and P. Kindler (1995), Sea-level highstand chronology from stable carbonate platforms (Bermuda and the Bahamas), *J. Coastal Res.*, *11*, 675–689.
Hearty, P. J., and S. L. Olson (2010), Geochronology, biostratigraphy, and changing shell morphology in the land snail subgenus Poecilozonites during the Quaternary of Bermuda, *Palaeogeogr. Palaeoclimatol. Palaeoecol.*, *293*, 9–29.
Hearty, P. J., H. L. Vacher, and R. M. Mitterer (1992), Aminostratigraphy and ages of Pleistocene limestones of Bermuda, *Geol. Soc. Am. Bull.*, *104*, 471–480, doi:10.1130/0016-7606(1992)104.
Hemming, S. R. (2004), Heinrich events: Massive late Pleistocene detritus layers of the North Atlantic and the global climate imprint, *Rev. Geophys.*, *42*, RG1005, doi:10.1029/2003RG000128.
Henkes, G. A., B. H. Passey, A. D. Wanamaker, E. L. Grossman, W. G. Ambrose, and M. L. Carroll (2013), Carbonate clumped isotope compositions of modern marine mollusk and brachiopod shells, *Geochim. Cosmochim. Acta*, *106*, 307–325.
Hervey, R. V., and US DOC; NOAA; NWS; National Data Buoy Center (2013), Meteorological and oceanographic data collected from the National Data Buoy Center Coastal-Marine Automated Network (C-MAN) and moored (weather) buoys during 2013-07 (NODC accession 0111971) Version 1.1. National Oceanographic Data Center, NOAA. Dataset.
Hill, J. C., and A. Condron (2014), Subtropical iceberg scours and meltwater routing in the deglacial western North Atlantic, *Nat. Geosci.*, *7*, 806–810, doi:10.1038/NGEO2267.
Hill, J. C., P. T. Gayes, N. W. Driscoll, E. A. Johnstone, and G. R. Sedberry (2008), Iceberg scours along the southern US Atlantic margin, *Geology*, *36*, 447–450.
Hodell, D. A., J. E. T. Channell, J. H. Curtis, and O. E. Romero (2008), Onset of "Hudson Strait" Heinrich events in the eastern North Atlantic at the end of the middle Pleistocene transition (~640 ka), *Paleoceanography*, *23*, PA4218, doi:10.1029/2008PA001591.
Hogg, N. G., and W. E. Johns (1995), Western boundary currents, *Rev. Geophys.*, 1311–1334, doi:10.1029/95RG00491.
Hwang, I., and P. L. Heller (2002), Anatomy of a transgressive lag: Panther Tongue Sandstone, Star Point Formation, central Utah, *Sedimentology*, *49*, 977–999.
Jones, D. S., D. F. Williams, and C. S. Romanek (1986), Life history of symbiont-bearing giant clams from stable isotope profiles, *Science*, *231*, 47–48.
Keigwin, L. D., and E. A. Boyle (1999), Surface and deep ocean variability in the northern Sargasso Sea during marine isotope stage 3, *Paleoceanography*, *14*, 164–170.
Kim, S., J. O'Neil, C. Hillaire-Marcel, and A. Mucci (2007a), Oxygen isotope fractionation between synthetic aragonite and water: Influence of temperature and Mg^{2+} concentration, *Geochim. Cosmochim. Acta*, *71*, 4704–4715.
Kim, S., A. Mucci, and B. E. Taylor (2007b), Phosphoric acid fractionation factors for calcite and aragonite between 25 and 75°C: Revisited, *Chem. Geol.*, *246*, 135–146, doi:10.1016/j.chemgeo.2007.08.005.
Kleypas, J. A., J. W. McManus, and L. A. B. Menez (1999), Environmental limits to coral reef development: Where do we draw the line?, *Am. Zool.*, *39*, 146–159, doi:10.1093/icb/39.1.146.
Kopp, R. E., F. J. Simons, J. X. Mitrovica, A. C. Maloof, and M. Oppenheimer (2009), Probabilistic assessment of sea level during the Last Interglacial stage, *Nature*, *462*, 863–867, doi:10.1038/nature08686.
Locarnini, R. A., et al. (2013), *World Ocean Atlas 2013, Volume 1: Temperature*, edited by S. Levitus and A. Mishonov, NOAA Atlas NESDIS 73, 40 pp.
Marino, G., E. J. Rohling, L. Rodriguez-Sanz, K. M. Grant, D. Heslop, A. P. Roberts, J. D. Stanford, and J. Yu (2015), Bipolar seesaw control on Last Interglacial sea level, *Nature*, *522*, 197–201.
Masson-Delmotte, V., et al. (2013), Information from paleoclimate archives, in *Climate Change 2013: The Physical Science Basis. Contribution of Working Group I to the Fifth Assessment Report of the Intergovernmental Panel on Climate Change*, edited by T. F. Stocker et al., pp. 383–464, Cambrige Univ. Press, Cambridge, U. K.
Muhs, D. R., K. R. Simmons, and B. Steinke (2002), Timing and warmth of the Last Interglacial period: New U-series evidence from Hawaii and Bermuda and a new fossil compilation for North America, *Quat. Sci. Rev.*, *21*, 1355–1383, doi:10.1016/S0277-3791(01)00114-7.
NEEM community members (2013), Eemian interglacial reconstructed from a Greenland folded ice core, *Nature*, *493*, 489–494.
O'Leary, M. J., P. J. Hearty, W. G. Thompson, M. E. Raymo, J. X. Mitrovica, and J. M. Webster (2013), Ice sheet collapse following a prolonged period of stable sea level during the Last Interglacial, *Nat. Geosci.*, *6*, 796–800.
Olson, S. L., and P. J. Hearty (2013), Periodicity of extinction and recolonization of the West Indian topshell *Cittarium pica* in the Quaternary of Bermuda (Gastropoda:Trochoidea), *Biol. J. Linn. Soc.*, *110*, 235–243.
Palter, J. B. (2015), The role of the gulf stream in European climate, *Annu. Rev. Mar. Sci.*, *7*, 113–37, doi:10.1146/annurev-marine-010814-015656.
Passey, B. H., and G. A. Henkes (2012), Carbonate clumped isotope bond reordering and geospeedometry, *Earth Planet. Sci. Lett.*, *351–352*, 223–236.
Petersen, S. V., and D. P. Schrag (2015), Antarctic ice growth before and after the Eocene-Oligocene transition: New estimates from clumped isotope paleothermometry, *Paleoceanography*, *30*, 1305–1317, doi:10.1002/2014PA002769.
Petersen, S. V., I. Z. Winkelstern, K. C. Lohmann, and K. W. Meyer (2016a), The effects of Porapak(™) trap temperature on $\delta^{18}O$, $\delta^{13}C$, and Δ_{47} values in preparing samples for clumped isotope analysis, *Rapid Commun. Mass Spectrom.*, *30*, 1–10, doi:10.1002/rcm.7438.
Petersen, S. V., C. R. Tabor, K. C. Lohmann, C. J. Poulsen, K. W. Meyer, S. J. Carpenter, J. M. Erickson, K. K. S. Matsunaga, S. Y. Smith, and N. D. Sheldon (2016b), Temperature and salinity of the Late Cretaceous Western Interior Seaway, *Geology*, *44*, 903–906.
Rahmstorf, S. (2002), Ocean circulation and climate during the past 120,000 years, *Nature*, *419*, 207–214, doi:10.1038/nature01090.
Rohling, E. J., K. Grant, C. Hemleben, M. Siddall, B. A. A. Hoogakker, M. Bolshaw, and M. Kucera (2008), High rates of sea-level rise during the Last Interglacial period, *Nat. Geosci.*, *1*, 38–42.
Rowe, M. P., and C. S. Bristow (2015), Sea-level controls on carbonate beaches and coastal dunes (eolianite): Lessons from Pleistocene Bermuda, *Geol. Soc. Am. Bull.*, *127*, 1645–1665, doi:10.1130/B31237.1.
Rowe, M. P., K. A. I. Wainer, C. S. Bristow, and A. L. Thomas (2014), Anomalous MIS 7 sea level recorded on Bermuda, *Quat. Sci. Rev.*, *90*, 47–59.
Ruddiman, W. F. (1977), Late Quaternary depostion of ice-rafted sand in the subpolar North Atlantic (lat 40° to 65°N), *Geol. Soc. Am. Bull.*, *88*, 1813–1827.
Schaefer, J. M., R. C. Finkel, G. Balco, R. B. Alley, M. W. Caffee, J. P. Briner, N. E. Young, A. J. Gow, and R. Schwartz (2016), Greenland was nearly ice-free for extended periods during the Pleistocene, *Nature*, *540*, 252–255.
Schauble, E. A., P. Ghosh, and J. M. Eiler (2006), Preferential formation of ^{13}C-^{18}O bonds in carbonate minerals, estimated using first-principles lattice dynamics, *Geochim. Cosmochim. Acta*, *70*, 2510–2529.
Schmidt, G. A., G. R. Bigg, and E. J. Rohling (1999), Global Seawater Oxygen-18 Database v1.21. [Available at http://data.giss.nasa.gov/o18data/.]

Schöne, B. R., and D. M. Surge (2012), Bivalve sclerochronology and geochemistry, in *Part N, Bivalvia, Revised*, *Treatise Online*, vol. 1, edited by P. Seldon and J. Hardesty chap. 14, pp. 1–24, Univ. of Kans., Lawrence.

Steinberg, D. K., C. A. Carlson, N. R. Bates, R. J. Johnson, A. F. Michaels, and A. H. Knap (2001), Overview of the US JGOFS Bermuda Atlantic Time-series Study (BATS): A decade-scale look at ocean biology and biogeochemistry, *Deep Sea Res., Part II*, *48*(8–9), 1405–1447, doi:10.1016/S0967-0645(00)00148-X.

Stevenson, S., B. S. Powell, M. A. Merrifeld, K. M. Cobb, J. Nusbaumer, and D. Noone (2015), Characterizing seawater oxygen isotopic variability in a regional ocean modeling framework: Implications for coral proxy records, *Paleoceanography*, *30*, 1573–1593, doi:10.1002/2015PA002824.

Stirling, C. H., T. M. Esat, K. Lambeck, and M. T. McCullock (1998), Timing and duration of the Last Interglacial: Evience for a restricted interval of widespread coral reef growth, *Earth Planet. Sci. Lett.*, *160*, 745–762.

Thomson, W. G., H. A. Curran, M. A. Wilson, and B. White (2011), Sea-level and ice-sheet instability during the Last Interglacial: New Bahamas evidence, *Nat. Geosci.*, *4*, 684–688.

Tripati, A. K., S. Sahany, D. Pittman, R. A. Eagle, J. D. Neelin, J. L. Mitchell, and L. Beaufort (2014), Modern and glacial tropical snowlines controlled by sea surface temperature and atmospheric mixing, *Nat. Geosci.*, *7*, 205–209.

Turney, C. S. M., and R. T. Jones (2010), Does the Agulhas Current amplify global temperatures during super-interglacials?, *J. Quat. Sci.*, *25*, 839–843.

Vacher, H. L. (1978), Hydrogeology of Bermuda—Significance of an across-the-island variation in permeability, *J. Hydrol.*, *39*, 207–226.

Vacher, H. L., and P. Hearty (1989), History of stage 5 sea level in Bermuda: Review with new evidence of a brief rise to present sea level during substage 5a, *Quat. Sci. Rev.*, *8*, 159–168, doi:10.1016/0277-3791(89)90004-8.

Vacher, H. L., P. J. Hearty, and M. P. Rowe (1995), Stratigraphy of Bermuda: Nomenclature, concepts and status of multiple systems of classification, *Geol. Soc. Spec. Pap.*, *300*, 271–294.

Vollbrecht, R. (1990), Marine and meteoric diagenesis of submarine Pleistocene carbonates from the Bermuda Carbonate Platform, *Carbonates Evaporites*, *5*, 13–96.

Welch, J. J. (2010), The "island rule" and deep-sea gastropods: Re-examining the evidence, *PLoS One*, *5*(1), e8776, doi:10.1371/journal.pone.0008776.

Winkelstern, I. Z., and K. C. Lohmann (2016), Shallow burial alteration of dolomite and limestone clumped isotope geochemistry, *Geology*, *44*, 463–466.

Zaarur, S., H. P. Affek, and M. T. Brandon (2013), A revised calibration of the clumped isotope thermometer, *Earth Planet. Sci. Lett.*, *382*, 47–57.